J|A|C|S
ARTICLES
Published on Web 10/26/2002

Molecular Structure of the Solvated Proton in Isolated Salts. Short, Strong, Low Barrier (SSLB) H-bonds

Daniel Stasko,[†] Stephan P. Hoffmann,[†] Kee-Chan Kim,[†] Nathanael L. P. Fackler,[†] Anna S. Larsen,[†] Tatiana Drovetskaya,[†] Fook S. Tham,[†] Christopher A. Reed,*[,†] Clifton E. F. Rickard,[‡] Peter D. W. Boyd,*[,‡] and Evgenii S. Stoyanov*[,§]

Contribution from the Departments of Chemistry, University of California, Riverside, California 92521-0403, and The University of Auckland, Private Bag, Auckland, New Zealand, and Boreskov Institute of Catalysis, Prospekt Lavrentieva, 5, Novosibirsk, 630090, Russia

Received December 6, 2001

Abstract: Large, inert, weakly basic carborane anions of the icosahedral type $CHB_{11}R_5X_6^-$ (R = H, Me; X = Cl, Br) allow ready isolation and structural characterization of discrete salts of the solvated proton, $[H(solvent)_x][CHB_{11}R_5X_6]$, (solvent = common O-atom donor). These oxonium ion Brønsted acids are convenient reagents for the tuned delivery of protons to organic solvents with a specified number of donor solvent molecules and with acidities leveled to those of the chosen donor solvent. They have greater thermal stability than the popular $[H(OEt_2)_2][BAr^F]$ acids based on fluorinated tetraphenylborate counterions because carborane anions can sustain much higher levels of acidity. When organic O-atom donors such as diethyl ether, tetrahydrofuran, benzophenone, and nitrobenzene are involved, the coordination number of the proton (x) in $[H(solvent)_x]^+$ is two. A mixed species involving the $[H(H_2O)(diethyl\ ether)]^+$ ion has also been isolated. These solid-state structures provide expectations for the predominant molecular structures of solvated protons in solution and take into account that water is an inevitable impurity in organic solvents. The O···O distances are all short, lying within the range from 2.35 to 2.48 Å. They are consistent with strong, linear O···H···O hydrogen bonding. Density functional theory calculations indicate that all $H(solvent)_2^+$ cations have low barriers to movement of the proton within an interval along the O···H···O trajectory, i.e., they are examples of so-called SSLB H-bonds (short, strong, low-barrier). Unusually broadened IR bands, diagnostic of SSLB H-bonds, are observed in these $H(solvent)_2^+$ cations.

Introduction

There is surprisingly little known about the detailed molecular structure of ionized acids in organic solvents. Although it is universally understood that writing H^+ is shorthand for a solvated proton, $H(solvent)_x^+$, the value(s) of x and the details of the coordination environment are often unspecified or unknown. This leads to incomplete descriptions of the mechanisms of acid-promoted and acid-catalyzed reactions, a matter of particular concern when contemplating the nature of active proton carriers in low dielectric media. The size and charge of a proton carrier is important throughout biology and can markedly affect the rates of protonation reactions when accessibility to the reacting center is a factor.[1−3] The unspecified nature of $H(solvent)_x^+$ also leads to an imprecise description of the phenomenon of solvent leveling of acidity because the basicity of an individual solvent molecule is a fundamentally different thermodynamic quantity than the solvation of a proton (as measured by pK_a). This is underscored by gas phase observations that proton affinities of solvent molecules do not correlate with hydrogen bond energies of the corresponding proton-bound dimers, $H(solvent)_2^+$.[4,5] The enthalpy of addition of a second solvent molecule to $H(solvent)^+$ is remarkably constant through a wide series of gas-phase bases, suggesting a unique stability for $x = 2$ in $H(solvent)_x^+$. This work probes this stability in solid-state structural studies.

By isolating and structurally characterizing a variety of salts containing representative $[H(solvent)_x]^+$ cations, we can expect to arrive at reasonable structural models for the nature of ionized acids in organic solvents.[6−9] This will be most favored when the counterion is large, weakly basic and weakly interacting − in short, as "innocent" as possible. Carborane anions of the type $1\text{-}H{-}CB_{11}R_5X_6^-$ (R = H, Me; X = Cl, Br)[10] (see Figure 1)

* To whom correspondence should be addressed. E-mail: chris.reed@ucr.edu.
[†] University of California, Riverside.
[‡] The University of Auckland.
[§] Boreskov Institute of Catalysis.

(1) Kramarz, K. W.; Norton, J. R. *Prog. Inorg. Chem.* **1994**, *42*, 1−65.
(2) Quadrelli, E. A.; Kraatz, H.-B.; Poli, R. *Inorg. Chem.* **1996**, *35*, 5154−5162.
(3) Evans, D. R.; Reed, C. A. *J. Am. Chem. Soc.* **2000**, *122*, 4660−4667.
(4) Lau, Y. K.; Saluja, P. P. S.; Kebarle, P. *J. Am. Chem. Soc.* **1980**, *102*, 7429−7433.
(5) Larson, J. W.; McMahon, T. B. *J. Am. Chem. Soc.* **1982**, *104*, 6255−6261.
(6) Klages, F.; Gordon, J. E.; Jung, H. A. *Chem. Ber.* **1965**, *98*, 3748−3764.
(7) Kolthoff, I. M.; Chantooni, M. K., Jr. *J. Am. Chem. Soc.* **1968**, *90*, 3320−3326.
(8) Olah, G. A.; White, A. M.; O'Brien, D. H. *Chem. Rev.* **1970**, *70*, 561−591.
(9) Stoyanov, E. S. *Phys. Chem. Chem. Phys.* **2000**, *2*, 1137−1145.
(10) Reed, C. A. *Acc. Chem. Res.* **1998**, *31*, 133−139.

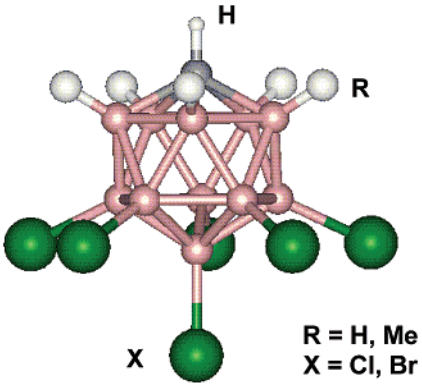

Figure 1. Icosahedral carborane anions used in this work, $CHB_{11}R_5X_6^-$ (R = H, Me; X = Cl, Br).

and fluorinated tetraphenylborates[11,12] (BAr^F) best fulfill this requirement. Carborane salts generally crystallize better than fluorinated tetraphenylborates because of a much lower tendency to form oily liquid clathrates.

A handful of X-ray structures of salts of protonated common organic solvents are known, suggesting a pattern of di-solvation of the proton. They include two examples of the $H(OEt_2)_2^+$ ion (with $Zn_2Cl_6^{2-}$ and perfluorinated tetraphenylborate counterions),[12,13] a number of $H(DMF)_2^+$ and $H(DMSO)_2^+$ structures,[14−17] one with the $H(MeOH)_2^+$ cation[18] and one with the $H(HOAc)_2^+$ cation.[19] A number of protonated organic molecules have been isolated from superacidic media and characterized by X-ray crystallography.[20−22] This latter class of cations provides models for mono-solvated protons but because they are produced in the presence of excess acid, they are unlikely to represent species present when acids are used in a bulk solvent. As discussed above, the basicity order for protonation of single organic molecules may differ significantly from the basicity order in bulk, because of the difference in coordination number of the proton.

A crucial role for single equivalents of water in organic media is also becoming apparent.[2,3,23] Adventitious water in organic solvents is essentially impossible to avoid, making the nature of mixed ions, $[H(solvent)_x(H_2O)_y]^+$, of particular interest. It is not widely recognized, but in isolation, H_3O^+ may be a superacid[24] having ca. 10^{12} greater acidity than the proton in water (as represented by the water-solvated $H_5O_2^+$ and $H_9O_4^+$ hydronium ions).[25−27]

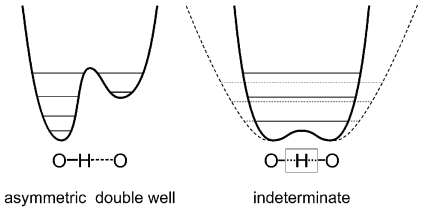

Figure 2. Schematic representation of proton potentials for two classes of O···H···O structure envisioned for $[H(solvent)_2]^+$ cations: (a) normal, asymmetric H-bonds, and (b) a family of flat-bottomed wells typical of short, strong H-bonds (SSHB).

The need for well-defined, solid-state structures is given added importance by the recent discovery of some notable effects in the solution IR spectra of $H(O\text{-donor})_2^+$ cations having weakly interacting anions. Stoyanov[9,28] has observed extensive broadening and shifting of ν(C═O) and ν(C−O) bands for a variety of di-solvated protons (solvent = acetone, ethanol, diethyl ether, and butyl acetate). These are related to IR continua observed earlier in a number of other strong H-bonded systems such as bis-formate[29] and bis-pyridine[30] proton complexes. The origin of this effect is now believed to be the response of these vibrations to the variable position of the proton within a spatial interval along the O···H···O trajectory. Rather than a double minimum, or a single minimum at the midway point, the potential energy curve for the proton is proposed to have a double minimum with a barrier so small that it is less than the energy of the ground state vibrational level (see Figure 2). Indeterminate positioning of the proton gives rise to a family of potential energy curves. These are referred to as SSLB H-bonds (SSLB = short, strong, low-barrier).[31−33] Strong H-bonds differ from typical, weak H-bonds most noticeably in their tendency toward low (or possibly zero) barriers to symmetrical positioning the H atom between the two electronegative atoms. On the basis of current understanding, two classes of $O\cdots H^+\cdots O$ hydrogen bonding can be envisaged for $H(solvent)_2^+$ species with O-donor solvents: (a) a localized, double-well potential arising from normal asymmetric H-bonding, and (b) a distribution of essentially flat wells arising in SSLB H-bonding (Figure 2). This has seen extensive investigation in $H(N\text{-donor})_2^+$ systems,[30] and in A−H···A$^-$ type systems that formally involve H-bonding of an acid HA to its anionic conjugate base A$^-$.[31−33] Cations of the type $H(O\text{-donor})_2^+$ provide a new class of H-bonds that might be expected to contain some of the strongest SSLB H-bonds. Considerable experimental debate[34−36] and theoretical attention[26,37−44] has been paid to strong H-bonding, but a complete understanding has yet to be gained. The existence of truly symmetrical O···H···O hydrogen bonds remains controversial.

A second thrust of this work is to build a repertoire of useful reagents for the stoichiometric delivery of protons having

(11) Brookhart, M.; Grant, B.; Volpe, A. F., Jr. *Organometallics* **1992**, *11*, 3920−3922.
(12) Jutzi, P.; Müller, C.; Stammler, A.; Stammler, H.-G. *Organometallics* **2000**, *19*, 1442−1444.
(13) Kolesnikov, S. P.; Lyudkovskaya, I. V.; Antipin, M. Y.; Struchkov, Y. T.; Nefedov, O. M. *Bull. Acad. Sci. USSR* **1985**, *34*, 74−80.
(14) Frydrych, R.; Muschter, T.; Brüdgam, I.; Hartl, H. *Z. Naturforsch.* **1990**, *45b*, 679−688.
(15) James, B. R.; Morris, R. H.; Kvintovics, P. *Can. J. Chem.* **1986**, *64*, 897−903.
(16) Cartwright, P. S.; Gillard, R. D.; Sillanpaa, E. R. J.; Valkonen, J. *Polyhedron* **1988**, *7*, 2143-2148.
(17) Rudnitskaya, O. V.; Buslaeva, T. M.; Koteneva, N. A.; Stash, A. I. *Russ. Chem. Bull.* **1994**, *43*, 1273−1274.
(18) Mootz, V. D.; Steffen, M. *Z. Anorg. Allg. Chem.* **1981**, *482*, 193−200.
(19) Bartmann, K.; Mootz, D. *Z. Anorg. Allg. Chem.* **1991**, *601*, 31−40.
(20) Laube, T. *Chem. Rev.* **1998**, *98*, 1277−1312.
(21) Olah, G. A.; Prakash, G. K. S.; Sommer, J. *Superacids*; John Wiley & Sons: New York, 1985.
(22) Minkwitz, R.; Reinemann, S. *Z. Anorg. Allg. Chem.* **1999**, *625*, 121−125.
(23) Bergquist, C.; Bridgewater, B. M.; Harlan, C. J.; Norton, J. R.; Friesner, R. A.; Parkin, G. *J. Am. Chem. Soc.* **2000**, *122*, 10 581−10 590.
(24) Farcasiu, D.; Hâncu, D. *J. Chem. Soc., Faraday Trans.* **1997**, *93*, 2161−2165.
(25) Eigen, M. *Angew. Chem., Int. Ed. Engl.* **1964**, *3*, 1−72.
(26) Zundel, G.; Shuster, P., Zundel, G. and Sandorfy, G., Ed.; North-Holland Publ. Co.: Amsterdam, 1976; Vol. 2, p 683.
(27) Xie, Z.; Bau, R.; Reed, C. A. *Inorg. Chem.* **1995**, *34*, 5403−5404.
(28) Stoyanov, E. S. *Mendeleev Communications* **1999**, 171−212.
(29) Spinner, E. *J. Am. Chem. Soc.* **1983**, *105*, 756−761.
(30) Rabold, A.; Bauer, R.; Zundel, G. *J. Phys. Chem.* **1995**, *99*, 1889−1895.
(31) Hibbert, F.; Emsley, J. *Adv. Phys. Org. Chem.* **1990**, *26*, 255−379.
(32) Perrin, C. L. *Science* **1994**, *266*, 1665−1668.
(33) Ash, E. L.; Sudmeier, J. L.; De Fabo, E. C.; Bachovchin, W. W. *Science* **1997**, *278*, 1128−1132.
(34) Frey, P. A.; Cleland, W. W. *Bioorg. Chem.* **1998**, *26*, 175−192.
(35) Perrin, C. L.; Nielson, J. B. *J. Am. Chem. Soc.* **1997**, *119*, 12 734−12 741.
(36) Howes, A. P.; Jenkins, R.; Smith, M. E.; Crout, D. H. G.; Dupree, R. *Chem. Commun.* **2001**, 1448−1449.

specified acidity and precisely defined solvation. Weighable acid reagents with weakly coordinating counterions such as the popular "BAr^F acid", $[H(OEt_2)_2][B(C_6H_3(CF_3)_2)_4]$,[11] have been widely used in organotransition metal chemistry to produce active cations for catalysis. However, this salt is barely thermally stable at room temperature. Because carborane anions are considerably more chemically inert than tetraphenylborates, reagents based on them should have longer shelf lives and should sustain much higher levels of acidity. This has, in fact, been demonstrated recently with the isolation of the superacids $[H(benzene)][CB_{11}H_6X_6]$[45] and $H(CB_{11}H_6X_6)$.[46] These well-defined, weighable salts are thermally stable to over 150 °C and have acidities many orders of magnitude higher than $[H(OEt_2)_2][BAr^F]$-type acids. Fluorinated tetraphenylborate anions cannot sustain acidity much higher than about H(mesitylene)$^+$,[45] being unstable with respect to boron−carbon bond cleavage in superacids or strong electrophiles. Attenuating the acidity of $H(CB_{11}H_6X_6)$ with a variety of solvents from benzene to water to produce reagents of the type $[H(solvent)_x][carborane]$, gives tuned Brønsted acid reagents spanning $>10^{16}$ range of acidity constants.

Results and Discussion

Ether Solvents. Bis-diethyl ether oxonium ions can be generated by a number of routes, one of the simplest being treatment of cesium carborane salts with anhydrous hydrogen chloride in dry diethyl ether solvent (1)

$$Cs(carborane) + HCl + 2Et_2O \rightarrow [H(OEt_2)_2][carborane] + CsCl \quad (1)$$

Colorless crystalline materials are readily isolated after removal of the CsCl by filtration. Alternatively, they can be made by treatment of [H(arene)][carborane] with ethers. Although somewhat hygroscopic, these salts do not show the room temperature thermal instability of the fluorinated tetraphenylborate analogues in solution or in the solid state. Thermogravimetric analysis of $[H(OEt_2)_2][CHB_{11}H_5Cl_6]$, **1**, shows stability in excess of 50 °C. Thermal stability is a function of the nucleophilicity of the accompanying solvent. Related salts that contain protonated solvents that are less nucleophilic than diethyl ether (e.g., arenes), are thermally stable to >150 °C.[45] The diethyl ether salts have good solubility in most organic solvents, including benzene. ^{1}H NMR spectroscopy confirms stoichiometry via integration of the anion and cation resonances. This is particularly accurate when the anions contain methyl groups. The acidic proton appears appropriately downfield[6,11−13] at 11−14 ppm, depending on conditions. Density functional calculations using the GIAO method predict a shift of 18.3 ppm. The less downfield shift observed experimentally suggests that second shell solvation effects, or possible tri-solvation of the proton, may be important in solution.

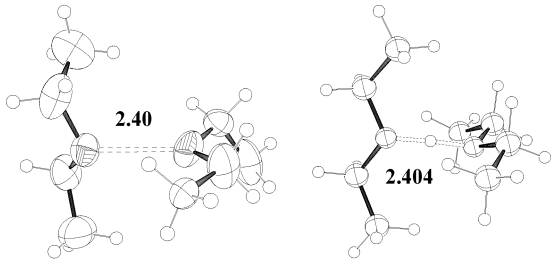

Figure 3. Perspective drawing of the cation in $[H(OEt_2)_2][CHB_{11}H_5Cl_6]$, **1**, (left) and the DFT calculated structure (right).

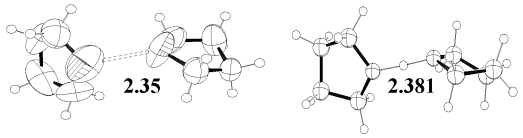

Figure 4. Perspective drawing of one of the two cations in the asymmetric unit of $[H(THF)_2][CHB_{11}H_5Br_6]$, **2**, (left) and the DFT calculated structure (right).

Another commonly used ether solvent, tetrahydrofuran (THF), can also be converted into a crystalline oxonium salt, despite the fact that THF polymerizes in strong acid. THF polymerization is a reversible, nearly thermoneutral transformation,[47] so that as long as the THF concentration is kept low and the temperature is ambient, the monomer is favored. Treatment of arenium ion carborane salts with a small excess of THF in benzene, followed by solvent evaporation, quantitatively generates the two-coordinate $H(THF)_2^+$ cation (2)

$$[H(arene)][carborane] + 2THF \rightarrow [H(THF)_2][carborane] + arene \quad (2)$$

Single-crystal X-ray structures were obtained for $[H(OEt_2)_2][CHB_{11}H_5Cl_6]$, **1**, and $[H(THF)_2][CHB_{11}H_5Br_6]$, **2**. The structures contain discrete anions and cations. No halogen atom of an anion approaches the midpoint of the O···O separation closer than 4.1 Å, and no H atom from a B−H bond approaches closer than 3.0 Å. The dimensions of the carborane are typical of the unperturbed anion. The location of the proton between the ether O atoms is very strongly implied by the short O···O separations averaging 2.40 Å in **1** and 2.360(10) Å and 2.349(13) Å in **2**, much shorter than the sum of two O-atom van der Waals radii (3.00 Å). In the case of **1**, the proton was located from the difference electron density map. It refined as two 50% occupied protons, each position shared by the two disordered cation conformers with O−H distances in the range 0.80−1.60 Å. This implies an asymmetric H-bond but disorder leaves doubt about the accuracy of all of the metrical data in the cation. Nevertheless, the shape of cation is clear. One of the conformers is shown in Figure 3 along with the DFT calculated structure. In **2**, there are two independent $H(THF)_2^+$ cations in the asymmetric unit. One of these is displayed along with the DFT calculated structure in Figure 4. Although near the limits of statistical significance, the C−O distances in the coordinated THF molecules [1.437(10)−1.455(10) Å] show an expected slight

(37) Hofacker, G. L.; Marechal, Y.; Ratner, M. A.; Schuster, P., Zundel, G. and Sandorfy, C., Ed.; North-Holland Publ. Co.: Amsterdam, 1976; Vol. 1, p 295.
(38) Romanovski, H.; Sobzik, L. *Chem. Phys.* **1977**, *19*, 361.
(39) Bratos, S.; Ratajczak, H. *J. Phys. Chem.* **1982**, *73*, 78.
(40) Tuckerman, M. E.; Marx, D.; Klein, M. L.; Parrinello, M. *Science* **1997**, *275*, 817−820.
(41) Marx, D.; Tuckerman, M. E.; Hutter, J.; Parrinello, M. *Nature* **1999**, *397*, 601−604.
(42) Jiang, J.-C.; Wang, Y.-S.; Chang, H.-C.; Lin, S. H.; Lee, Y. T.; Niedner-Schatteburg, G.; Chang, H.-C. *J. Am. Chem. Soc.* **2000**, *122*, 1398−1410.
(43) Kumar, G. A.; McAllister, M. A. *J. Am. Chem. Soc.* **1998**, *120*, 3159−3165.
(44) Schiøtt, B.; Iversen, B. B.; Madsen, G. K. H.; Bruice, T. C. *J. Am. Chem. Soc.* **1998**, *120*, 12 117−12 124.
(45) Reed, C. A.; Fackler, N. L. P.; Kim, K.-C.; Stasko, D.; Evans, D. R.; Boyd, P. D. W.; Rickard, C. E. F. *J. Am. Chem. Soc.* **1999**, *121*, 6314−6315.
(46) Reed, C. A.; Kim, K.-C.; Bolskar, R. D.; Mueller, L. *Science* **2000**, *289*, 101−104.

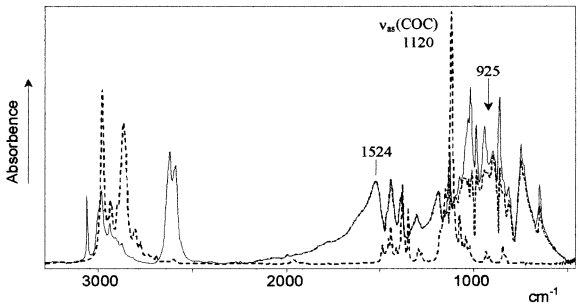

Figure 5. Infrared spectrum (KBr) of $[H(OEt_2)_2][CHB_{11}H_5Cl_6]$, **1** (solid line), with anion bands at 3058s, 2016s 1135s, 1031s, 1015s, 988s, 946s, 870s, 819m, 750m, 650m cm^{-1} subtracted (dashed line). These spectra are compared to free Et_2O (dotted line) whose sharp ν_{as}C−O−C at 1120 cm^{-1} is lost in **1**.

lengthening from those in a THF lattice solvate [1.41(1) Å].[48] The average O···O separations of 2.40 Å in **1** and 2.355(13) Å in **2** can be compared to the value of 2.396(4) Å reported for $[H(OEt_2)_2]_2[Zn_2Cl_6]$[13] and 2.445(9) Å for $[H(OEt_2)_2][B(C_6F_5)_4]$.[12] The values calculated for **1** and **2** via DFT methods are 2.404 and 2.381 Å respectively. Higher thermal parameters in the atoms of the cations relative to those of the anions in the published structures suggest caution in drawing any conclusions about differences in the experimental data. All of the values are within 5 standard deviations of 2.40 Å and are among the shortest known for O···H···O systems.

The IR spectra of **1** and **2** show the very broad and intense bands associated with the O−H−O fragment, typical of strong hydrogen bonds.[49,50] As illustrated in Figure 5 for the $H(OEt_2)_2^+$ cation, the band assigned to ν_{as}(O−H−O) is seen as a very broad feature centered at ca. 1000 cm^{-1} and that assigned to δ(O−H−O) is centered at 1524 cm^{-1}. The shapes of these bands, particularly the lower energy band, are distorted by resonance effects leading to so-called "transparent windows". These appear as irregular oscillations in the lower energy band of **1** (Figure 5) and as dips in the spectrum of **2** centered at 1484, 1366, and 1165 cm^{-1} (Figure S2). This effect is commonly observed in crystalline species with very strong H-bonds.[51−53] The spectrum of the cation in **1** fully coincides with that of $[H(OEt_2)_2][FeCl_4]$ in CCl_4 solution.[9] This indicates that the anion influence is minor, consistent with the well-separated ions seen in the crystal structures, and weak ion pairing in solution. Nevertheless, the carborane anion ν(B−H) stretching bands at ca. 2600 cm^{-1} are split into two bands reflecting asymmetry in its immediate environment. The center of mass of the broad ν_{as}(O−H−O) and δ(O−H−O) bands in **2** appear to have slightly lower frequencies than in **1**, consistent with the shorter O···O distance in **2** and a slightly stronger H-bond with THF relative to diethyl ether.

A striking peculiarity of the IR spectra of **1** and **2** is the disappearance of the ν_{as}(C−O−C) bands of the ethers, expected as strong, sharp bands ca. 50−100 cm^{-1} lower than in the free ethers (1120 cm^{-1} in diethyl ether). These bands are presumably broadened and obscured by ν_{as}(O−H−O), whose resonance distortion does not allow deconvolution of underlying bands. Their disappearance has been explained in terms of delocalization of the proton on the flat bottom of a potential well between the O···O atoms.[9] It is consistent with an indeterminate position of H^+ within an interval along the O···H···O trajectory, giving rise to a family of potential energy curves (Figure 2b). It is a particularly dramatic case of inhomogeneous line broadening.

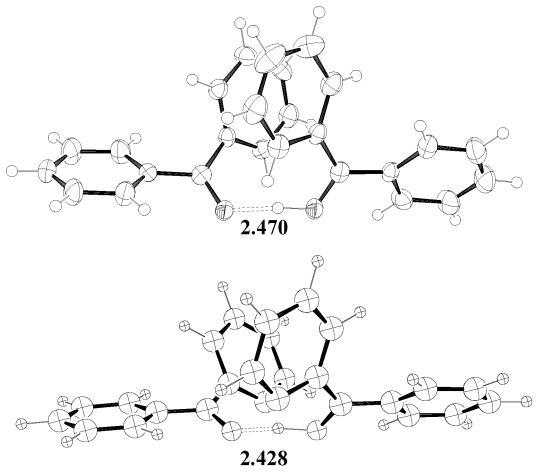

Figure 6. Perspective drawing of the cation in $[H(benzophenone)_2][CHB_{11}H_5Cl_6]$, **3**, (above) and the DFT calculated structure (below).

DFT calculations indicate that the proton is centered between the two O atoms in these bis-ether cations. However, excursions of the proton 0.25 Å either side of center point along the O···O trajectory lead to only small increases in the total energy of the system (<0.02 kcal). Taken together, the experimental and theoretical data are consistent with SSLB hydrogen bonds having a roughly centered but somewhat indeterminate position for the proton. The crystal lattice appears to impose a small degree of asymmetry.

Protonated Benzophenone. Ketones are a common class of organic solvents for carrying out acid-catalyzed reactions. Although we were unable to obtain single crystals of an acetone oxonium salt, we have been able to isolate suitable crystals of $[H(benzophenone)_2][CHB_{11}H_5Cl_6]$, **3**. The structure contains discrete cations and anions.

As shown in Figure 6, benzophenone forms a two-coordinate structure with a short O···O separation of 2.470(3) Å. There are clear indications of localization of the proton toward one component of the dimer. The acidic proton was located in the difference electron density map and refined with 100% occupancy in an asymmetric site (O···H = 0.09 and 1.50 Å). One C═O bond is slightly elongated relative to the other by 0.026(4) Å and this is further reflected in the adjacent C−C bonds to the phenyl groups which are correspondingly shorter (1.457(5) versus 1.480(5) Å), consistent with developing quinoidal character. Density functional calculations mirror these results giving an O···O separation of 2.428 Å and a difference of 0.02 Å between the two carbonyl C═O distances (Figure 6). Nevertheless, the IR spectrum of **3** is not classical. The usually sharp and intense ν(C═O) band of the carbonyl group (1650 cm^{-1} in free benzophenone) is not readily identified. As shown in Figure 7, a very broad absorption is present across the entire spectral region below 2000 cm^{-1}. Unlike the spectra of the ether species, the broad bands due to ν_{as}(O−H−O) and δ(O−H−O)

(47) Dreyfuss, P.; Dreyfuss, M. P. *Adv. Polymer Sci.* **1967**, *4*, 528−590.
(48) Cotton, F. A.; Ilsley, W. H. *Inorg. Chem.* **1981**, *20*, 572−578.
(49) Librovich, N. B.; Šakun, V. P.; Sokolov, N. D. *Chem. Phys.* **1979**, *39*, 351−366.
(50) Sokolov, N. D.; Vener, M. V.; Savelev, V. A. *J. Mol. Struct.* **1988**, *177*, 93−110.
(51) Videnova-Adrabinska, V.; Baran, J.; Ratajczak, H. *Spectrochim. Acta A* **1986**, *42*, 641−648.
(52) Videnova-Adrabinska, V. *J. Mol. Struct.* **1990**, *237*, 367−388.
(53) Baran, J.; Ilczyszyn, M. M.; Jakubas, R.; Ratajczak, H. *J. Mol. Struct.* **1991**, *246*, 1−12.

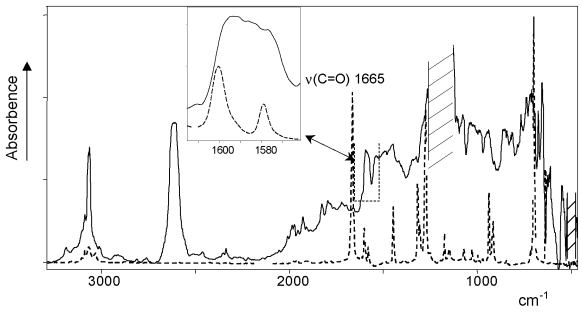

Figure 7. IR spectrum of $[H(benzophenone)_2][CHB_{11}H_5Cl_6]$, **3**, pressed between Teflon film (solid line) compared to free benzophenone (dotted line). The inset shows the probable region of coordinated ν(C═O). The crossed regions indicate where Teflon is not transparent.

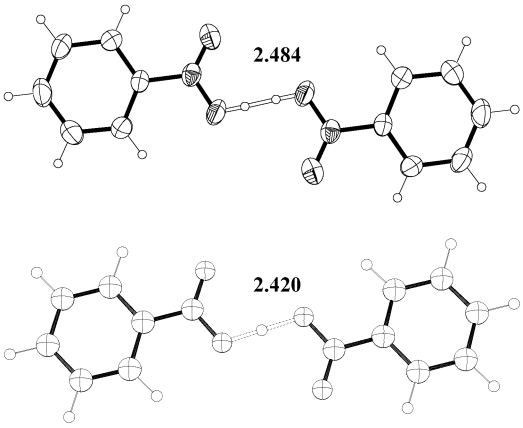

Figure 8. Perspective drawing of the cation in $[H(nitrobenzene)_2][CHB_{11}H_5Cl_6]$, **4**, (above) and the slightly asymmetric DFT calculated structure (below).

are not separated. Perhaps this reflects the asymmetry of the O···H···O moiety seen in the crystal structure. It is not possible to subtract bands due to ν_{as}(O−H−O) and δ(O−H−O) in order to locate the carbonyl stretch. Possibly ν(C═O) is associated with two or more somewhat broad, weak bands in the 1600−1572 cm^{-1} region, overlapping with ν(C−C) phenyl ring vibrations (see insert of Figure 7).

Taken all together, the data are consistent with an intrinsically asymmetric H-bond but nevertheless one that is short, strong and with low barrier between the inequivalent minima. When the proton is constrained to a centered position between the O atoms in DFT calculations, the energy is virtually indistinguishable from that of the fully relaxed structure. This suggests that crystal site asymmetry provides a deciding bias for the average position of the proton. It suggests that second shell solvation effects may play a parallel role in solution.

Protonated Nitrobenzene. The least basic solvent used in this study was nitrobenzene. Crystals of $[H(nitrobenzene)_2][CHB_{11}H_5Cl_6]$, **4**, were isolated from nitrobenzene solution. As shown in Figure 8, the close approach of O atoms at 2.484(3) Å indicates that protonation occurs in monodentate fashion on the nitro groups, giving a symmetrical dimer. The O···O separation is the longest observed in the present studies. As seen in Table 1, the dimensions of the protonated nitro group are similar to those in nitrobenzene·$AlCl_3$[54] suggesting similar acidity. The coordinated N−O bond length is ca. 0.05 Å elongated relative to free nitrobenzene while the noncoordinated N═O bond is ca. 0.02 Å shortened. Although a symmetrical location for the proton is required by crystallographic site

Table 1. Selected Interatomic Distances (Å) for Free and Monodentate-coordinated Nitrobenzene

Compound	C—N	N═O	N—O	Ref.
	1.465	1.223	1.229	[a]
	1.480	1.196	1.242	[b]
	1.429	1.198	1.279	Ref. 54
 experimental	1.438	1.200	1.274	This work
 calculated	1.420 1.430	1.199 1.200	1.28 1.27	This work

[a] Boese, R.; Blaser, D.; Nussbaumer, M.; Krygowski, T. M. *Struct. Chem.* **1992**, *3*, 363−368. [b] Rack, J. J.; Hurlburt, P. K.; Kellett, P. J.; Luck, J. S.; Anderson, O. P.; Strauss, S. H. *Inorg. Chim. Acta* **1996**, *242*, 71−79.

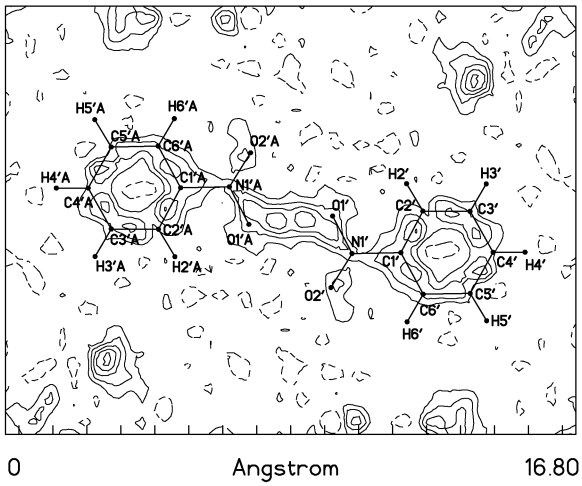

Figure 9. Difference electron density map of the $H(nitrobenzene)_2^+$ cation in **4**.

symmetry, refinement with an H atom at the inversion center led to a site occupation factor of only 39% (compared to 50% theoretical). This suggested a 2-fold static disorder of asymmetric H-bonds about the center of symmetry, or the variable position of the proton in an interval between the O atoms, biased away from the centroid. The difference electron density map is shown in Figure 9. The structure refined successfully with the former model although this does not rule out the latter. The thermal ellipsoids of the coordinated O atoms are normal so if the proton takes a variable position (as indicated by the IR data below) the X-ray data are not revealing on this point. DFT calculations lead to a very slightly asymmetric structure (Figure 8) with an O···O distance of 2.420 Å. The coordinated N−O distances are 1.273 and 1.281 Å, whose average is very close to the experimental distance of 1.274 Å. Calculated excursions of the proton through the central position indicate that the barrier is low (<0.1 kcal/mol). We conclude that an asymmetric H-bond is favored but that a distribution of locations in an interval between the O atoms cannot be ruled out. X-ray crystallography

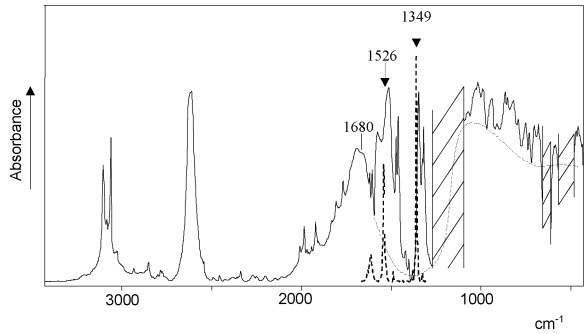

Figure 10. Infrared spectrum of $[H(nitrobenzene)_2][CHB_{11}H_5Cl_6]$, **4**, pressed between Teflon film (solid line) compared to free nitrobenzene (dotted line). The dashed line indicates an approximation to the bands associated with ν_{as}(O−H−O) and δ(O−H−O). The crossed regions indicate where Teflon is not transparent.

gives information on the location of electron density not the nuclei. Lacking core electrons and being highly acidic, the actual location of a proton is very much open to debate.

The distance of H^+ to the other, formally nonprotonated O atom of nitrobenzene is short: ca. 2.23 Å (or 2.37 Å to the centroid). Thus, the coordination of nitrobenzene appears to be slightly bidentate. This is supported by the difference electron density map (Figure 9) and suggests an explanation for the relatively long O···O separation (2.47 Å). Secondary H-bonding weakens the primary H-bonding. It also provides a model for second shell effects in the solution structures of $H(solvent)_2^+$ systems.[55]

The bond length changes of the coordinated nitrobenzene lead to ready prediction of the IR spectrum. The *longer* the coordinated N−O bond, the more $\nu_s(NO_2)$ should *decrease* in frequency relative to free nitrobenzene. The *shorter* the uncoordinated N═O bond, the more $\nu_{as}(NO_2)$ should *increase* in frequency. This has, in fact, been observed in aliphatic nitro compounds having monodentate coordination to $AlCl_3$.[54]

The IR spectrum of **4** is shown in Figure 10. Strong sharp $\nu(NO_2)$ bands at 1526/1513 and 1348 cm^{-1} are assigned to small amounts of free nitrobenzene adhering to the surface crystals or produced by reaction of $[H(nitrobenzene)_2][CHB_{11}H_5Cl_6]$ with traces of water. Of all the species studied, the nitrobenzene compound is the most sensitive to moisture or errant nucleophiles. For example, it reacts rapidly with KBr, in a pellet and even as a Nujol mull between KBr windows, to liberate nitrobenzene whose $\nu_{as}(NO_2)$ frequencies vary by ca. 10 cm^{-1} depending on the environment. This is why a Teflon film had to be used to obtain an authentic spectrum of **4**. The problem of reaction with the matrix or window material may explain why coordinated nitrobenzene has sometimes been reported to show insignificant shifts in the νNO bands.[56] We assign a new, somewhat broad band at 1325 cm^{-1} to $\nu_s(NO_2)$. It's companion $\nu_{as}(NO_2)$ band would be expected at a frequency higher than that of free nitrobenzene, i.e., higher than 1526 cm^{-1}. This region is obscured but, by allowing water to partially decompose the sample and taking difference spectra, a somewhat broad band at 1567 cm^{-1} could be identified. This is tentatively assigned to $\nu_{as}(NO_2)$.

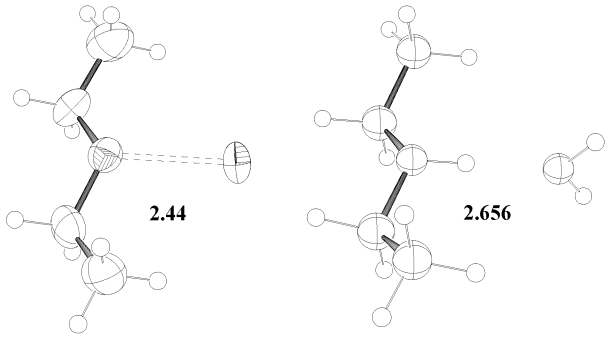

Figure 11. Perspective drawing of the cation in of $[H(Et_2O)(H_2O)][CHB_{11}H_5Cl_6]$, **5**, (left) and its DFT calculated structure (right).

Thus, as with the benzophenone structure, the nitrobenzene cation shows a considerable loss of intensity of the stretching vibrations of bonds adjacent to SSLB H-bonds, suggesting some degree of indeterminate position for the proton. This is not inconsistent with the X-ray structure determination.

Mixed $[H(diethyl\ ether)(H_2O)]^+$ Cation. Adventitious water in our solvents led to the serendipitous growth of single crystals of $[H(OEt_2)(H_2O)][CHB_{11}H_5Cl_6]$, **5**, although this species can be prepared rationally with controlled amounts of water in well-dried solvents. Despite the opportunity for extended H-bonding involving the water ligand, discrete cations are found in the crystal structure. There are four structurally similar cations in the crystallographic asymmetric unit.

The cation is intrinsically unsymmetrical, so the question of location of the proton is not one of centering, but one of competition between water and ether. The difference electron density map and the distinct nonlinearity of the H^+−O−H bond angles to H_2O indicate that the proton is closer to the ether. Theory favors a bias toward methanol in the gas-phase structure of $[H(MeOH)(H_2O)]^+$.[57] Nevertheless, the chemical behavior of traces of water in solvents indicates that $H(H_2O)(solvent)^+$ is more stable than $H(solvent)_2^+$. Solvation energies presumably play a role in this. The O···O separations of 2.404(16), 2.441(8), 2.448(9), and 2.469(9) Å in **5** (average 2.44 Å) are toward the long end of those in the chemically symmetrical cations (2.35−2.48 Å) but are nevertheless short. This suggests that they remain in the overall category of strong linear O···H···O bonds. These expectations are borne out by DFT calculations where comparison is made in Figure 11. Within the organic moieties, bond length comparisons between mixed species and its symmetrical $H(OEt_2)_2^+$ counterpart cannot be made at a meaningful level of statistical accuracy.

Conclusions

With weakly interacting anions, a notably consistent pattern of di-solvation of the proton by O-donor organic solvents has emerged from this work. This should be taken as the predominant form of an ionized acid in solvents having O-atom donors, and may be the same with other heteroatom donors. It contrasts with C-protonation of arene solvents where all the evidence to date points toward mono-solvation of protons in σ-complexed arenium ions, $H(arene)^+$.[45,58]

(54) Lanfranchi, M.; Pellinghelli, M. A.; Predieri, G.; Bigi, F.; Maggi, R.; Sartori, G. *J. Chem. Soc., Dalton Trans.* **1993**, *9*, 1463−1464.
(55) Stoyanov, E. S.; Vorob′eva, T. P.; Smirnov, I. V. *Zh. Struct. Chim.* **2002**, accepted for publication.
(56) Driessen, W. L.; Van Geldrop, L. M.; Groeneveld, W. L. *Rec. Trav. Chim.* **1970**, *89*, 1271.
(57) Chang, H.-C.; Jiang, J.-C.; Hahndorf, I.; Lin, S. H.; Lee, Y. T.; Chang, H.-C. *J. Am. Chem. Soc.* **1999**, *121*, 4443−4450.
(58) Reed, C. A.; Kim, K.-C.; Stoyanov, E. S.; Stasko, D.; Tham, F. S.; Mueller, L. J.; Boyd, P. D. W. *J. Am. Chem. Soc.*, submitted for publication.

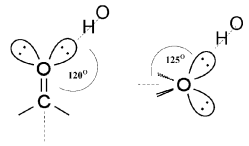

Figure 12. Lone pair directionality expected for sp^2 and sp^3 hybridized oxygen atoms.

H(O-donor)$_2^+$ systems all have short O···O separations (2.35−2.48 Å) indicative of strong, linear, H-bonding. DFT calculations indicate that symmetrical structures can exist since all have low barrier H-bonds although they are not majority species. In all cases, broadened IR bands provide strong evidence for an indeterminate position of the proton within an interval between the donor atoms. The distribution of structures favors asymmetry.

The present structures allow comment on the VSEPR notion that protonation occurs on sp^2- and sp^3-oriented lone pairs of oxygen atoms (Figure 12). Expectations that carbonyl and nitro groups protonate on lone pairs at approximately 120° are, in fact, borne out by the data. The C═O−H angles (assuming linear O···H···O bonds) are 120° and 123° to benzophenone in **3** and the N═O−H angle is 111° to nitrobenzene in **4**. The same angles calculated with density functional theory are 120° and 113° respectively. In neutral systems, where H-bonding is weaker, these angles tend to be greater than 120°. The most common angle from the crystallographic database is 128°, the average is 130°, but there is considerable spread.[59]

Although the sp^2 model is a fairly good guide to structure in unsaturated compounds, the sp^3 model for lone pairs in ethers fairs poorly. Oxonium ions have considerably flattened pyramidal geometries relative to that predicted from sp^3 tetrahedrality. This is measured as the dihedral angle between the O···H···O vector and the C−O−C plane. The ideal is 125° for sp^3 hybridization (109° bond angles). These dihedral angles are 140°, 144°, 147°, and 169° (average 150°) to Et_2O in **1**, 130°, 145°, 147°, and 149° (average 140°) to THF in **2**, and 130°, 141°, 141°, and 145° (average 136°) to Et_2O in **5**. Calculated with density functional theory these angles are 145°, 153°, and 140° respectively. This suggests that the extensive flattening of the pyramidal geometry is intrinsic rather than of crystal packing origin. The remaining lone pair on the oxygen atom appears to have significantly diminished sp^3 character and, thus, diminished basicity. This is relevant to the concept of superelectrophiles in postulated dicationic species such as diprotonated ethers, $R_2OH_2^{2+}$, whose structural basis is presently confined to in vacuo calculation.[60]

In the second thrust of this work, we have shown that a variety of [H(solvent)$_2^+$][carborane$^-$] salts can be prepared, providing convenient weighable sources of Brønsted acid reagents having a wide range of selected acidities and excellent thermal stabilities. The molecular weights are convenient for accurate stoichiometric control of acidification in small scale reactions. These salts complement, and in a number ways eclipse, the popular [H(OEt$_2$)$_2$][BAr^F] acids based on fluorinated tetraphenylborate anions. With the recent report of a less expensive preparation of the parent $CB_{11}H_{12}^-$ ion,[61] they should soon become cheaper and more available. Acidity can be readily tuned over a much wider range of solvents with carborane counterions than tetraphenylborates.

The nucleophilicities of the solvent and anion that accompany the delivery of a proton to a substrate are often important considerations. The choice can be now made between two O-donor solvent molecules, an arene[45,58] and the unsolvated pure acid, H(carborane).[46] The redox inertness of a carborane anion and its exceedingly low nucleophilicity allows delivery of exceptionally "clean" protons to substrates at controlled acidity. There are potential applications to reactive cation chemistry across the periodic table.

Experimental Section

All manipulations were carried out under dry conditions using Schlenkware or an inert atmosphere glovebox (H_2O, O_2 < 0.5 ppm). Carborane anions,[62−64] protonated arene salts,[45,58] and $H_9O_4^+$ salts[27] were prepared as previously described. Solvents were dried by standard methods.[65] IR spectra were run on a Shimadzu 8300 FT-IR spectrometer in the range 4000−400 cm^{-1} (32 scans, resolution 2 cm^{-1}). Samples were prepared as both KBr pellets and as thin wafers pressed between 13 micron FEP Teflon films to ensure there was no reaction with pellet media. Reaction of **4** with KBr was very rapid.

[H(OEt$_2$)$_2$][CHB$_{11}$H$_5$Cl$_6$], 1. Into a 100 mL round-bottom flask flushed with HCl, a solution of Cs(CHB$_{11}$H$_5$Cl$_6$) (430 mg, 0.89 mmol) in diethyl ether (20 mL) was introduced via cannula . An immediate decrease of pressure and the formation of a white precipitate of CsCl indicated reaction. After cooling on ice for 1 h, the supernatant was carefully transferred under argon via cannula to a new Schlenk flask. The volume of the solution was reduced by half under vacuum, causing crystal formation. This was completed by cooling at 10 °C for 24 h and then at −10 °C for 3 weeks. Large colorless crystals of **1** suitable for X-ray were collected by decantation (335 mg, 85%). Anal. Calcd. for $C_9H_{27}B_{11}Cl_6O_2$: C, 21.66; H, 5.45; N, 0.0. Found: C, 21.49; H, 5.45; N, 0.05. ^{1}H NMR (C_6D_6): 13.8 (br, 1H, H$^+$), 4−2 (br, 5H, BH), 3.32 (q, 8H, CH_2), 1.71 (s, 1H, HCB), 0.78 (t, 12H, CH_3) ppm. IR (KBr, Figure 5) cation: 3000m, 2984s, 2938m, 2907w,br, 2872w, 1524s,vbr, 925vs,vbr; anion: 3059s, 2620s, 2589s, 1133m, 1031m, 1019s, 988m, 944s, 864s, 816w, 750, 650m cm^{-1}. TGA: 5 deg/min, 7% loss by 120 °C beginning at 50 °C.

[H(OEt$_2$)$_2$][CHB$_{11}$Me$_5$Br$_6$], 1b. 1b and other [H(OEt$_2$)$_2$][carborane] salts were prepared by the following general procedure. To diethyl ether (0.03 mL) and toluene was added [H(toluene)][carborane] (20−100 mg). After dissolution, the solvents were removed under reduced pressure to give essentially quantitative yields of white solids. ^{1}H NMR (C_6D_6) of **1b**: 11.7 (br, 1H, H$^+$), 3.22 (q, 8H, CH_2), 1.40 (s, 1H, HCB), 0.75 (t, 12H, CH_3), 0.60 (s, 15H, MeB) ppm. IR (KBr, Fig. S1) cation: see **1**; anion: 3017m, 2948m, 2829w, 1315vs, 1174s, 992s, 979s, 965s, 933m, 896s. TGA: 5 deg/min, 9% loss by 140 °C beginning at 70 °C.

[H(THF)$_2$][CHB$_{11}$H$_5$Br$_6$], 2. This was prepared in manner similar to **1b** using THF in place of diethyl ether. Anal. Calcd. for $C_9H_{23}B_{11}Br_6O_2$: C, 14.19; H, 3.04; N, 0.0. Found: C, 14.30; H, 3.09; N, 0.10. ^{1}H NMR (C_6D_6): 14.8 (br, 1H, H$^+$), 3.60 (m, 8H, OCH_2), 4−2 ppm (br, 5H, BH) 1.90 (s, 1H, HCB), 1.30 (m, 8H, CH_2) ppm. IR [KBr, Figure S2 (see the Supporting Information)] cation: 2988m, 2954m, 2933w, 2909m, 2880m, 1048vs,vbr; anion: 3051s, 2602s, 990s, 858s cm^{-1}. TGA: 5 deg/min, 4% loss by 170 °C beginning at 90 °C.

[H(THF)$_2$][CHB$_{11}$Me$_5$Br$_6$], 2b. 2b was prepared in the same manner as **2**. ^{1}H NMR (C_6D_6): 14.8 (br, 1H, H$^+$), 3.58 (m, 8H, OCH_2), 1.4 (s, 1H, HCB), 1.30 (m, 8H, CH_2), 0.55 (s, 15H, MeB) ppm. IR (KBr) Figure S3 (see the Supporting Information): cation: see **2**; anion: see **1b**. TGA: 5 deg/min, 4% loss by 140 °C beginning at 90 °C.

[H(Ph$_2$CO)$_2$][CHB$_{11}$H$_5$Cl$_6$], 3. This was prepared in a manner similar to **1b** using benzophenone in place of diethyl ether. Anal. Calcd. for $C_{27}H_{27}B_{11}Cl_6O_2$: C,45.35; H, 3.80; N, 0.0. Found: C, 44.95; H,

(59) Platts, J. A.; Howard, S. T.; Bracke, B. R. F. *J. Am. Chem. Soc.* **1996**, *118*, 2726−2733.
(60) Olah, G. A. *Angew. Chem., Int. Ed. Engl.* **1993**, *32*, 767−922.
(61) Franken, A.; King, B. T.; Rudolph, J.; Rao, P.; Noll, B. C.; Michl, J. *Collect. Czech. Chem. Commun.* **2001**, *66*, 1238−1249.

Table 2. Final Unit Cell Parameters and Structural Data for Compounds **1**−**5**

	1	2	3	4	5
crystal system	monoclinic	monoclinic	triclinic	monoclinic	monoclinic
space group	$P2_1/c$	P 2_1/n	P-1	$P2_1/m$	P 2_1/n
a (Å)	7.6777(4)	12.15240(10)	9.9028(5)	7.6653(8)	23.374(5)
b (Å)	23.5020(13)	24.9529(2)	13.8281(7)	19.583(2)	15.107(4)
c (Å)	13.5215(7)	17.1935(2)	13.9213(7)	9.0121(9)	23.804(5)
α (°)	90	90	68.2140(10)	90	90
β (°)	90.7730(10)	108.350(1)	74.9370(10)	91.987(2)	99.907(10)
γ (°)	90	90	84.967(2)	90	90
Vol. $Å^3$	2439.6(2)	4948.52(8)	1709.28(15)	1352.0(2)	8280(3)
Z	4	8	2	2	16
Fw	498.92	761.64	715.10	596.90	442.81
D_c (g/cm^3)	1.358	2.045	1.389	1.466	1.421
Temp. (K)	198(2)	203(2)	198(2)	213(2)	170(2)
GOF on F^2	1.020	1.022	1.021	1.040	1.013
R1 ($I>2\sigma I$)	0.0409	0.0496	0.0536	0.0382	0.0534
R1 (all)	0.0666	0.1025	0.0922	0.0545	0.1248
wR2 ($I>2\sigma I$)	0.0949	0.0887	0.1236	0.0962	0.1025
wR2 (all)	0.1055	0.1067	0.1410	0.1064	0.1248
Diff. pk/ho ($e/Å^3$)	0.649/−0.219	0.920/−0.961	1.371/−0.342	0.887/−0.448	0.303/−0.316

3.86; N, 0.06. ^{1}H NMR (C_6D_6): 7.42 (d, 4H, *o*-phenyl), 7.16 (m, 2H, *p*-phenyl), 7.02 (m, 4H, *m*-phenyl), 3.5−1.5 (br, 5H, BH), 1.60 (s, 1H, HCB) ppm. IR (Teflon, Figure 7) cation: 3186w, 3144w, 3101w, 3085w, ∼1584w, ∼1490s,vbr, ∼1100vs,vbr, cm^{-1}; anion: see compound **1**.

$[H(NO_2C_6H_5)_2][CHB_{11}H_5Cl_6]$, 4. This was prepared by condensing ca. 0.5 mL of nitrobenzene onto $H(CHB_{11}H_5Cl_6)$ (0.15 g) and evaporating the solvent under vacuum. Anal. Calcd. for $C_{13}H_{17}B_{11}Cl_6N_2O_4$: C, 26.15; H, 2.87; N, 4.69. Found: C, 25.95; H, 3.00; N, 4.81. IR (Teflon): cation: 3102s, 3082w, 3035w, 3025w, 1670vs,vbr, 1567w, 1325m, ∼1070vs.vbr; anion: see **1**.

$[H(OEt_2)(H_2O)][CHB_{11}H_5Cl_6]$, 5. To a suspension of $[H_9O_4][CHB_{11}H_5Cl_6]$ (0.02 g, 0.05 mmol) in benzene was added 0.3 mL of diethyl ether. The mixture was agitated for 30 min., and the solvent removed under vacuum. The solid was rinsed with hexanes and dried under vacuum. ^{1}H NMR (C_6D_6): 11−12 (br, 3H, H_3O^+), 3.22 (q, 4H, CH_2), 1.5−4 (br, 5H, BH), 1.55 (s, 1H, HCB), 0.71 (t, 6H, CH_3) ppm. IR [KBr, Figure S4 (see the Supporting Information)]: cation: 3476br, 2983m, 1520m, 1442m, 1483m cm^{-1}; anion: see **1**.

$[H(OEt_2)(H_2O)][CHB_{11}Me_5Br_6]$, 5b. To a suspension of $[H_9O_4][CHB_{11}Me_5Br_6]$ (0.40 g, 0.26 mmol) in benzene was added 0.3 mL of diethyl ether. The mixture was agitated for 30 min., and the solvent removed under vacuum. The mixture was redissolved in benzene and separated from a white solid contaminant (ascribed to the $H_5O_2^+$ salt). The product was obtained by fractional crystallization from benzene (approximately 3 times) until $H_5O_2^+$ bands were absent from the sample. The solid was rinsed with hexanes and dried under vacuum. ^{1}H NMR (75% C_6D_6 / 25% $CDCl_3$): 3.22 (q, 4H, CH_2), 1.40 (s, 1H, HCB), 0.90 (t, 6H, CH_3), 0.30 (s, 15H, MeB) ppm. IR [KBr, Figure S5 (see the Supporting Information)] cation: see **5**; anion: see **1**.

X-ray Structure Determinations. Single crystals of **1** were grown from diethyl ether, **2** from THF-benzene, **3** from toluene, **4** from very concentrated nitrobenzene and **5** from diethyl ether. X-ray data were collected as previously described for **1, 3** and **4**[66] and for **2** and **5**.[45] Structures were solved and refined by standard methods. A summary is given in Table 2. Details are provided in the Supporting Information.

Density Functional Calculations. These were carried out using the Gaussian 98 program.[67] Full geometry optimizations were carried out on each of the solvated proton complexes at the B3P86/6-311+G** level. Examinations of the energy profiles were performed by systematic variation of an O−H internal coordinate in the $O-H^+-O$ moiety with optimization of all other geometric parameters at each point. Tables of optimized geometries are available in the Supporting Information.

Acknowledgment. We thank Professor Robert Bau for assistance with crystal-structure determinations and Professors Peter Schwerdfeger, Graham Bowmaker, and Zuowei Xie for helpful discussions. This work was made possible by the National Institutes of Health (Grant No. GM 23851), the National Science Foundation (Grant No. CHE 0095206), The University of Auckland Research Committee, and by Award No. RC1-2399-NO-02 of the U.S. Civilian Research & Development Foundation for the Independent States of the Former Soviet Union.

Supporting Information Available: Infrared spectra, tables of optimized atomic coordinates from Density Functional calculations, and full crystallographic details: atomic coordinates, anisotropic displacement coefficients, bond lengths, and angles, H atom coordinates, packing diagrams, and atom numbering schemes (pdf). This material is available free of charge via the Internet at http://pubs.acs.org.

JA012671I

(62) Plesek, J.; Jelinek, T.; Drdakova, E.; Hermanek, S.; Stibr, B. *Collect. Czech. Chem. Commun.* **1984**, *49*, 1559−1562.
(63) Jelinek, T.; Baldwin, P.; Scheidt, R. W.; Reed, C. A. *Inorg. Chem.* **1993**, *32*, 1982−1990.
(64) Stasko, D.; Reed, C. A. *J. Am. Chem. Soc.* **2002**, *124*, 1148−1149.
(65) Perrin, D. D.; Armarego, W. L. F.; Perrin, D. R. *Purification of Laboratory Chemicals*; 2nd ed.; Pergamon Press Ltd.: Sydney, 1980.
(66) Larsen, A. S.; Tham, F. S.; Reed, C. A. *J. Am. Chem. Soc.* **2000**, *122*, 7264−7272.
(67) Frisch, M. J.; Trucks, G. W.; Schlegel, H. B.; Scuseria, G. E.; Robb, M. A.; Cheeseman, J. R.; Zakrzewski, V. G.; Montgomery, J. A.; Stratmann, R. E.; Burant, J. C.; Dapprich, S.; Millam, J. M.; Daniels, A. D.; Kudin, K. N.; Strain, M. C.; Farkas, O.; Tomasi, J.; Barone, V.; Cossi, M.; Cammi, R.; Mennucci, B.; Pomelli, C.; Adamo, C.; Clifford, S.; Ochterski, J.; Petersson, G. A.; Ayala, P. Y.; Cui, Q.; Morokuma, K.; Malick, D. K.; Rabuck, A. D.; Raghavachari, K.; Foresman, J. B.; Cioslowski, J.; Ortiz, J. V.; Stefanov, B. B.; Liu, G.; Liashenko, A.; Piskorz, P.; Komaromi, I.; Gomperts, R.; Martin, R. L.; Fox, D. J.; Keith, T.; Al-Laham, M. A.; Peng, C. Y.; Nanayakkara, A.; Gonzalez, C.; Challacombe, M.; Gill, P. M. W.; Johnson, B. G.; Chen, W.; Wong, M. W.; Andres, J. L.; Head-Gordon, M.; Replogle, E. S.; Pople, J. A. *Gaussian 98*, Revision A.7; Gaussian, Inc.: Pittsburgh, PA, 1998.